

Fast Sign Retrieval via Sub-band Convolution: An Elementary Extension of Binary Classification

Fuma Ito¹, Chihiro Tsutake¹, Keita Takahashi¹, and Toshiaki Fujii¹

¹ Department of Information and Communication Engineering, Nagoya University,
Furo-cho, Chikusa-ku, Nagoya, 464-8603, Japan

Abstract

To efficiently compress the sign information of images, we address a sign retrieval problem for the block-wise discrete cosine transformation (DCT): reconstruction of the signs of DCT coefficients from their amplitudes. To this end, we propose a fast sign retrieval method on the basis of binary classification machine learning. We first introduce 3D representations of the amplitudes and signs, where we pack amplitudes/signs belonging to the same frequency band into a 2D slice, referred to as the sub-band block. We then retrieve the signs from the 3D amplitudes via binary classification, where each sign is regarded as a binary label. We implement a binary classification algorithm using convolutional neural networks, which are advantageous for efficiently extracting features in the 3D amplitudes. Experimental results demonstrate that our method achieves accurate sign retrieval with an overwhelmingly low computation cost.

Keywords. Image coding, discrete cosine transform, sign information, phase retrieval, binary classification, deep neural network.

1 Introduction

Compressing sign information in data is a challenging problem, and it plays a fundamental role in a wide range of research fields. In image coding, a large number of bits, approximately 20% of the total bits, generated by an image encoder are allocated for the signs, as reported in [1]. Against this background, many previous works [2–5] have developed sign compression methods within the context of image coding, specifically focusing on compressing signs of discrete cosine transform (DCT) [6] coefficients.

To reduce the bits for signs, in our earlier work [7, 8], we slightly modified a standardized image encoder and decoder, such as JPEG, as summarized in Fig. 1. In the encoder, DCT coefficients of an image are separated into the signs, referred to as the *true signs*, and amplitudes; the latter is encoded in the first place. The encoder locally reconstructs the signs using a *sign retrieval* method whose algorithmic procedure is shared with the decoder. Instead of encoding the true signs, we encode residuals (XORs) between the true signs and retrieved ones. In the decoder, an image is decoded by following the reverse path of the encoding process, where the XORs between the residuals and retrieved signs perfectly reconstruct the true signs. If the signs are retrieved correctly

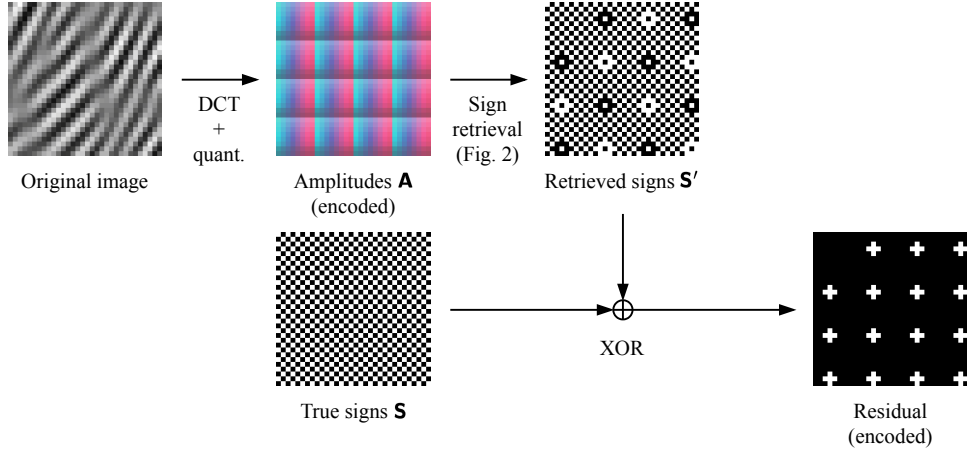
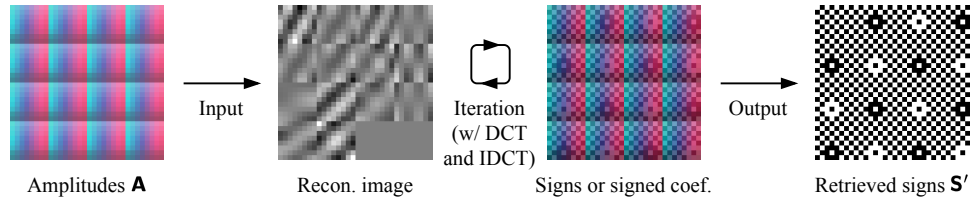
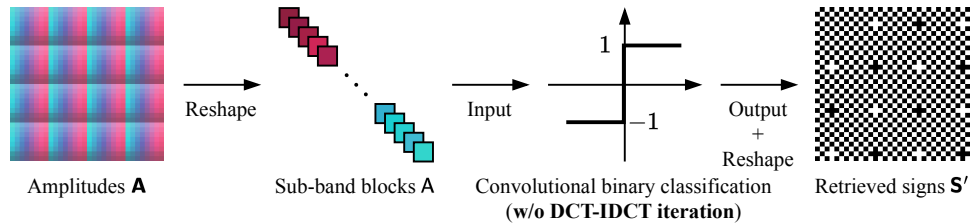


Figure 1: Encoding process in [7].



(a) Previous methods [7, 8, 13, 14]



(b) Proposed

Figure 2: Sign retrieval methods.

to some extent, the residuals have many zeros but few ones; the residuals can be compressed using entropy coding methods, e.g., [9–12]. Therefore, the accuracy of the retrieved signs is crucial for successful sign compression.

Various sign retrieval methods have been proposed, as summarized in Fig. 2a. To the best of our knowledge, all of the previous methods, without exception, are based on iterative optimization. For example, in [7, 8], an image and signed DCT coefficients are alternatively retrieved, and the signs of the retrieved coefficients are extracted. In [14], the signs are regarded as variables and are optimized in an iterative manner. Previous methods have demonstrated the ability to accurately retrieve a large portion of the signs; for example, as reported in [8], roughly 75% of the total signs can be retrieved. However, these methods come at an excessive computation cost, primarily due

to computing the DCT and the inverse DCT (IDCT) for each iteration. For example, as reported in [8], it takes approximately 10 [s] to retrieve 256×256 signs, making sign retrieval impractical for real-time encoding and decoding scenarios.

To accelerate the speed of sign retrieval, we propose a fast method **without the DCT-IDCT iteration**, which is summarized in Fig. 2b. Unlike previous methods, our method retrieves the signs in a direct manner, where sign retrieval is regarded as a variant of a binary classification problem. We first introduce 3D representations of the amplitudes and signs, where we pack amplitudes/signs belonging to the same frequency band into a 2D slice, referred to as the *sub-band block* [2]. We then retrieve the signs from the 3D amplitudes via binary classification, where each sign is regarded as a binary label. We implement a binary classification algorithm using convolutional neural networks (CNNs), which are advantageous for efficiently extracting features in the 3D amplitudes. Experimental results demonstrate that our method achieves accurate sign retrieval with an overwhelmingly low computation cost: only **0.93%** of the execution time taken for previous methods.

Limitations: Throughout this paper, we utilize constant-size blocks, as was done in JPEG [15], which is not compatible with the variable-size ones in state-of-the-art image coding standards such as high-efficiency video coding (HEVC) [16] and versatile video coding (VVC) [17]. However, we believe that our promising results (discussed in Section 4) will contribute to further advancements in the field of image coding.

2 Related work

2.1 Sign retrieval

The sign-retrieval-based method [7], illustrated in Fig. 1, is a seminal work in sign compression. Sign retrieval is known as a special instance of phase retrieval: namely, determining the signs ± 1 is identical to retrieving their phases, 0 and π , on the Gaussian plane. Therefore, sign retrieval has typically been addressed on the basis of phase retrieval approaches. Tsutake et al. [7] proposed an ℓ_1 -norm minimization method, motivated by the prior works on phase retrieval [18, 19]. Lin et al. [13] proposed a similar method based on total variation minimization. Suzuki et al. [8] proposed a CNN-based least squares method. Sidiropoulos et al. [14] proposed a quadratic programming method. All of these methods, without exception, retrieve the signs via iterative processes, as illustrated in Fig. 2a. For example, an image and signed DCT coefficients are alternatively computed in [7, 8], similar to the Gerchberg-Saxton method [20] and Fienup method [21]. The Frank-Wolfe method [22], utilized in [14], is another example, which is a variant of a gradient method and computes the DCT to determine the descent direction. Due to the iterative nature, the DCT and IDCT should be conducted in each iteration, leading to significant computation costs.

2.2 Sign compression without sign retrieval

Ponomarenko et al. [3] proposed a prediction-based method similar to the sign retrieval-based method [7], where the amplitudes are encoded before sign compression. Their method predicts the

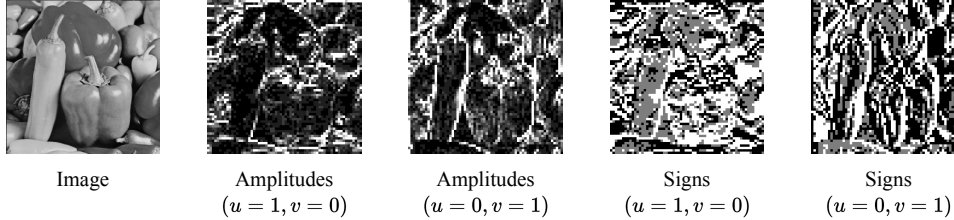


Figure 3: Sub-band blocks obtained from image, $\times 8$ enlarged. Larger amplitudes are represented by brighter luminance. Positive and negative signs are represented by white and black, respectively. Black regions in amplitudes and gray ones in signs correspond to non-significant coefficients.

signs block-by-block by solving an amplitude-constrained combinatorial problem, where the signs that minimize an objective function are searched. To reconstruct the true signs at the decoder, residuals between the true signs and predicted ones are encoded. As reported in [3], the bit amount for the residuals is 60–85% of that for the true signs. Subsequent works, such as [23–25], have been developed to enhance the accuracy and computation efficiency.

Clare et al. [26] proposed a sign compression method, known as sign data hiding, which is a fundamental component in state-of-the-art image coding standards, HEVC [16] and VVC [17]. This method allows us to skip encoding a single sign of DCT coefficients for each block. The decoder can compensate for the missing sign by executing a parity check. As reported in [26], sign data hiding achieves a BD-rate [27] (a rate-distortion metric) of approximately -0.6% compared to the HM 4.0 anchor¹. Sign data hiding has been improved in subsequent works, such as [28–30], where the encoding of multiple signs per block can be skipped.

Tu and Tran [2] proposed a sign compression method inspired by sub-band coding [31, 32]. They constructed the so-called sub-band blocks, which include amplitudes/signs belonging to the same frequency band, and the true signs are encoded and decoded in the sub-band domain. Figure 3 shows examples of sub-band blocks obtained from an image, where u and v represent frequency indices along the horizontal and vertical directions, respectively. As can be seen, each element is strongly correlated with its spatial and sub-band neighbors. This remarkable statistical feature of the sub-band representation is imported into our method.

3 Proposed method

3.1 Notations

A scalar variable and a scalar-valued function are denoted by a regular typeface. A constant value is denoted by a capital case. A 3D tensor, 3D-tensor-valued function, and their elements are denoted by a sans-serif typeface. A 4D tensor and its elements are denoted by a bold sans-serif typeface. A set is denoted by a Greek letter.

As shown in Figs. 1 and 2, the amplitudes of quantized DCT coefficients are denoted by a 4D tensor \mathbf{A} , and the true and retrieved signs are denoted by \mathbf{S} and \mathbf{S}' , respectively. Figure 4a illustrates

¹<https://hevc.hhi.fraunhofer.de>

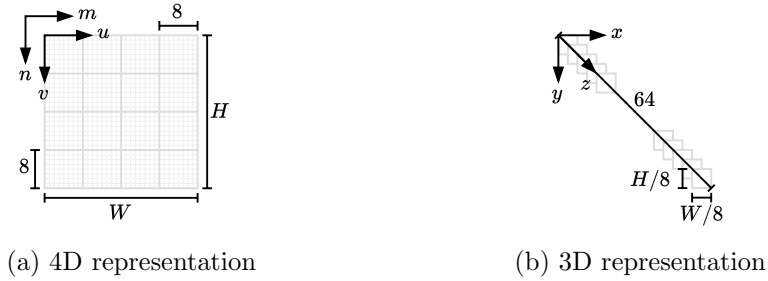


Figure 4: Coordinate systems.

the coordinate system of \mathbf{A} , \mathbf{S} , and \mathbf{S}' . The width and height of an image are denoted by W and H , respectively. The block size is fixed to 8×8 . Frequency indices of the DCT basis function are denoted by $u \in [0, 8)$ and $v \in [0, 8)$. Block indices are denoted by $m \in [0, W/8)$ and $n \in [0, H/8)$. The (u, v) -th element in the (m, n) -th block of \mathbf{A} , \mathbf{S} , and \mathbf{S}' is denoted by $[\cdot]_{u,v,m,n}$. As shown in Fig. 4b, we introduce 3D representations of \mathbf{A} , \mathbf{S} , and \mathbf{S}' , which are denoted by \mathbf{A} , \mathbf{S} , and \mathbf{S}' , respectively. Their axes are x , y , and z , and the (x, y, z) -th element is denoted by $[\cdot]_{x,y,z}$.

3.2 Sign retrieval via sub-band convolution

To accelerate sign retrieval, we propose a fast method without the DCT-IDCT iteration, which is summarized in Fig. 2b. Our method retrieves the signs based on binary classification machine learning. Because processing 4D tensors as they are requires a large computational cost, we reshape the 4D amplitudes and signs into 3D ones, as follows:

$$\mathbf{A}_{x,y,z} = \mathbf{A}_{u(z),v(z),m(x),n(y)} \quad (1)$$

$$\mathbf{S}_{x,y,z} = \mathbf{S}_{u(z),v(z),m(x),n(y)}, \quad (2)$$

where $u(z) = \lfloor z/8 \rfloor$, $v(z) = z \bmod 8$, $m(x) = x$, and $n(y) = y$. The amplitudes/signs belonging to the $(u(z), v(z))$ -th frequency band are packed in the z -th 2D slice, referred to as the sub-band block, and the 3D tensors contain all the 64 sub-band blocks, as shown in Figure 3. We simply stack these 64 sub-bands along the z dimension; consideration of even/odd symmetry of the DCT kernels might lead to a better method for handling these sub-bands, but we leave it as the future work. The effectiveness of the reshaping process will be demonstrated in Section 4.2.

We aim to reconstruct the signs \mathbf{S} from the 3D amplitudes \mathbf{A} via binary classification, where each sign is regarded as a binary label. We implement a binary classification algorithm using CNNs, which have the capability to efficiently extract features in \mathbf{A} along the spatial and sub-band directions. Table 1 shows the network architecture of our CNN, where I represents the number of layers. The Conv- i has a 3D kernel of the size $3 \times 3 \times C$ (3×3 : spatial kernel size and C : the number of input channels) for each output channel, where all the channels (frequency sub-bands) can interact together in each convolution step. The spatial kernel size 3×3 in the sub-band domain corresponds to 24×24 pixels in the original image domain; thus, a sufficiently large spatial neighbor is considered in each convolution step. Our CNN maps the 3D amplitudes \mathbf{A} into a sign tensor of the size $W/8 \times H/8 \times 63$, where the number of channels, 63, corresponds to the AC components.

We denote the inferred signs by $F(\mathbf{A}, \Theta)$, where Θ represent a set of learnable parameters including convolution kernels and biases.

The training procedure is as follows. Let $\Phi = \{(\mathbf{A}[k], \mathbf{S}[k]) : k \in [0, K)\}$ be a set of 3D amplitudes and 3D signs for training, where K denotes the number of data. We define the empirical risk

$$r(\Phi, \Theta) = \frac{1}{WH} \frac{1}{K} \sum_{x,y,z} \sum_k l(F_{x,y,z}(\mathbf{A}[k], \Theta), \mathbf{S}_{x,y,z}[k]), \quad (3)$$

where l is a loss function. We obtain the optimal parameter, denoted by $\tilde{\Theta}$, by minimizing the empirical risk:

$$\tilde{\Theta} = \underset{\Theta}{\operatorname{argmin}} r(\Phi, \Theta). \quad (4)$$

The solution to (4) is obtained using the Adam optimizer.

The loss function l in (3) is defined as follows. Let

$$b(\mathbf{S}_{x,y,z}) = \begin{cases} 1 & \text{if } \mathbf{S}_{x,y,z} = 1 \\ 0 & \text{otherwise} \end{cases} \quad (5)$$

be a zero-one representation of the true sign $\mathbf{S}_{x,y,z}$. We utilize the binary cross-entropy function as the loss function:

$$l(F_{x,y,z}, \mathbf{S}_{x,y,z}) = -b(\mathbf{S}_{x,y,z}) \log(F_{x,y,z}) - (1 - b(\mathbf{S}_{x,y,z})) \log(1 - F_{x,y,z}), \quad (6)$$

where (\mathbf{A}, Θ) of $F_{x,y,z}$ has been omitted for notation convenience. If the (x, y, z) -th amplitude is zero, we set the corresponding loss value to 0.

At the test phase, we obtain the retrieved signs by thresholding $F_{x,y,z}(\mathbf{A}, \Theta^*)$ as follows.

$$\mathbf{S}'_{x,y,z} = \begin{cases} +1 & \text{if } F_{x,y,z} \geq 1/2 \\ -1 & \text{otherwise} \end{cases} \quad (7)$$

Let $x(m) = m$, $y(n) = n$, and $z(u, v) = 8u + v$. A 4D representation of the retrieved signs can be computed as follows.

$$\mathbf{S}'_{u,v,m,n} = \mathbf{S}'_{x(m),y(n),z(u,v)} \quad (8)$$

We encode the residuals between the true signs \mathbf{S} and the retrieved ones \mathbf{S}' , as shown in Fig. 1.

4 Experimental results

4.1 Configuration

For training our CNN, we randomly cropped $K = 6,056$ images with a size of $W \times H = 512 \times 512$ from the CLIC 2020 dataset [33]. The bit-depth was 8 bits/pixel, and each pixel value was normalized within the range 0–1. We applied block-wise DCT to the images. We quantized the DCT coefficients using the quality factor (QF) of 75. We reshaped the 4D amplitudes and signs in accordance with (1) and (2); as a result, we obtained 3D tensors with a size of $W/8 \times H/8 \times 64 =$

Table 1: Network architecture.

Layer	Conv-0	...	Conv- i	...	Conv- I
Ker. size	$3 \times 3 \times 64$...	$3 \times 3 \times 128$...	$3 \times 3 \times 128$
In/out ch.	64/128	...	128/128	...	128/63
Act.	ReLU	...	ReLU	...	Sigmoid
Input	3D amp. A	...	Conv $i - 1$...	Conv $I - 1$

Table 2: Computing environment.

CPU	Intel Core i9-13900KF
Main memory	32 GB
OS	Ubuntu 20.04 LTS
Language & framework	Python 3.10.11 & PyTorch 1.13.1

$64 \times 64 \times 64$. We utilized the Adam optimizer with the learning rate 2×10^{-4} . The batch size and the number of epochs were 256 and 15,000, respectively. We varied the number of convolution layers I (Table 1) from 2 to 8. For convenience, we refer to the proposed method trained on the above configuration as the *sub-band convolution method*.

To evaluate the effectiveness of the reshaping processes in (1) and (2), we employed the following alternative approach, referred to as the *naive method*. We treated the collection of all amplitudes (or signs) depicted in Fig. 4a as a plane with dimensions $W \times H = 512 \times 512$. We reconstructed the sign planes from the amplitude planes, where we nullified the reshaping process in the sub-band convolution method. To adapt the network architecture for planes, we changed the input channel of Conv-0 and the output channel of Conv- I to 1. For fair comparison, the training process follows the same configuration as that employed in the sub-band convolution method.

For evaluation, we sampled 60 images from the CLIC 2021 dataset [33], which were not included in the training dataset. The DCT coefficients of the images were quantized with QFs of 15, 30, 45, 60, 75, and 90. The signs were retrieved using our methods (sub-band convolution and naive) and previous methods [7, 8, 13]; the latter were iterative methods requiring per-iteration DCT and IDCT (discussed in Section 2.1). For the previous methods, we changed the maximum number of iterations from 1 to 200. All the experiments were conducted on the computing environment in Table 2; all the methods were executed using the same CPU.

To quantify the accuracy of the retrieved signs, we define the following recovery rate:

$$\frac{\#(\text{correctly retrieved signs of AC coefficients})}{\#(\text{signs of AC coefficients})},$$

where the signs of DC coefficients and non-significant coefficients are excluded. We also measured the execution time [s] of all the methods for sign retrieval.

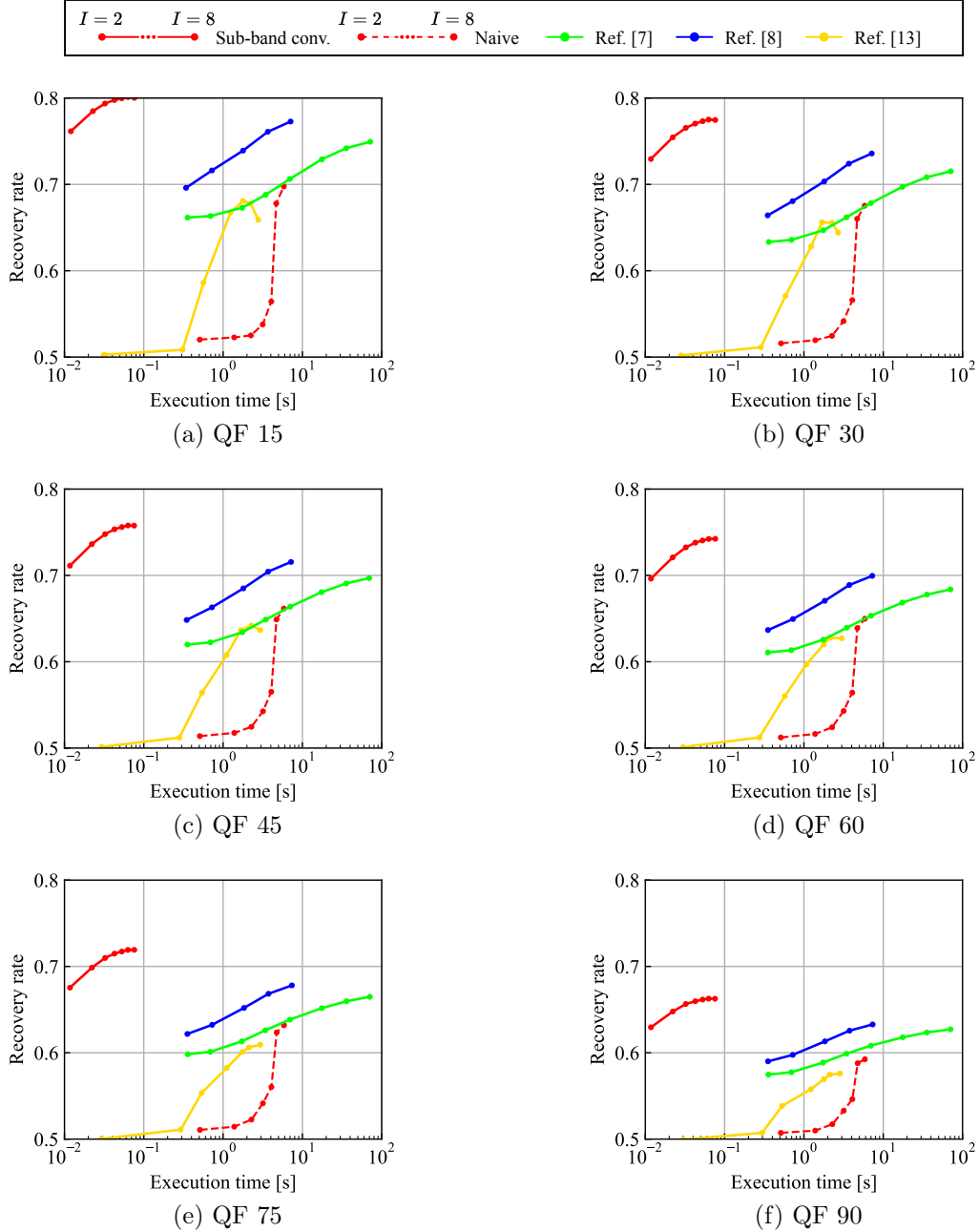
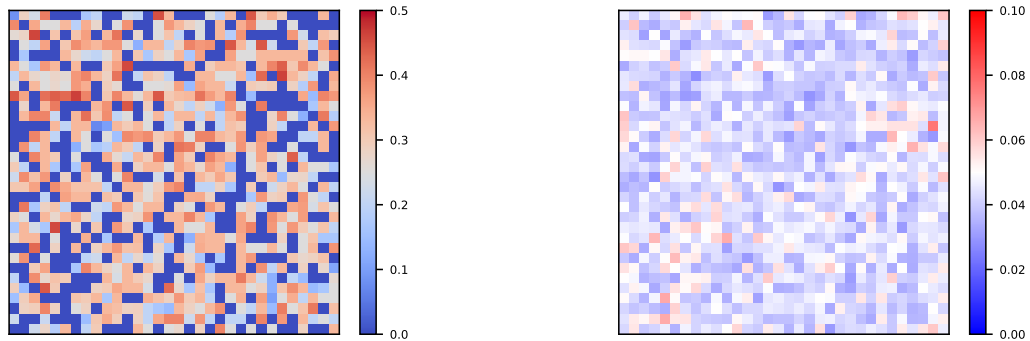


Figure 5: Recovery rate against execution time.

4.2 Results

Figure 5 shows recovery rates against execution times, which were averaged over all blocks in the 60 test images. The seven points in our method represent results for different values of $I \in [2, 8]$, while the points in the previous methods represent results for different iteration counts. For all the QFs, the sub-band convolution method perfectly outperformed the previous methods in terms of the



(a) Worst

(b) Variance

Figure 6: Heat maps of recovery rates for each block.

recovery rate while achieving the shortest execution time. Specifically, the execution time for the maximum recovery rate was 6.74×10^{-2} s on average, i.e., **0.93%** of 7.24 s for the state-of-the-art method [8]. It is worth noting that the sub-band convolution method also outperformed the naive approach, which demonstrates the effectiveness of the reshaping process.

Remark 1: We report recovery rates for each block to investigate their biases. We cropped 256×256 regions from the 60 test images and fed amplitudes of their DCT coefficients (QF 75) into our CNN ($I = 8$). We computed the average of recovery rates for each block and obtained the worst value and the variance over the 60 images. Figure 6 illustrates the results. We observe that there are clusters of low recovery rates and high variance values at the boundaries.

Remark 2: For all the methods, the recovery rates tend to increase as QF decreases. For small QFs, significant DCT coefficients are concentrated at the low frequency bands, which simplifies sign retrieval. Therefore, all the methods achieved high recovery rates at small QFs. In contrast, for large QFs, DCT coefficients are distributed across all the frequency bands, which increases the difficulty of sign retrieval; all the methods thus obtained low recovery rates.

5 Conclusion

In this work, we addressed a sign retrieval problem for the block-wise discrete cosine transformation (DCT): reconstruction of the signs of DCT coefficients from their amplitudes. To accelerate sign retrieval, we proposed a fast sign retrieval method without the DCT-IDCT iteration, where the signs are retrieved based on binary classification machine learning. We first introduced 3D representations of the amplitudes and signs and then implemented our method by convolutional neural networks, which are advantageous for extracting features in the 3D amplitudes. Our future work will include the extension of our method to the current state-of-the-art image coding standards, which utilize variable-size blocks. We also need to consider other transformations than the DCT, e.g., the discrete sine transform and low-frequency non-separable secondary transform [34]. We believe that this research direction has the potential to enhance the efficiency of image coding.

References

- [1] J. Sole, R. Joshi, N. Nguyen, T. Ji, M. Karczewicz, G. Clare, F. Henry, and A. Duenas, “Transform coefficient coding in HEVC,” *IEEE Transactions on Circuits and Systems for Video Technology*, vol. 22, no. 12, pp. 1765–1777, 2012.
- [2] C. Tu and T. D. Tran, “Context-based entropy coding of block transform coefficients for image compression,” *IEEE Transactions on Image Processing*, vol. 11, no. 11, pp. 1271–1283, 2002.
- [3] N. N. Ponomarenko, A. V. Bazhyna, and K. O. Egiazarian, “Prediction of signs of DCT coefficients in block-based lossy image compression,” *SPIE 6497, Image Processing: Algorithms and Systems V*, 2007.
- [4] J. Koyama, A. Yamori, K. Kazui, S. Shimada, and A. Nakagawa, “Coefficient sign bit compression in video coding,” *Picture Coding Symposium*, 2012.
- [5] O. Miroshnichenko, M. Ponomarenko, V. Lukin, and K. Egiazarians, “Compression of signs of DCT coefficients for additional lossless compression of JPEG images,” *International Symposium on Electronic Imaging: Image Processing: Algorithms and Systems XVI*, 2018.
- [6] N. Ahmed, T. Natarajan, and K. R. Rao, “Discrete cosine transform,” *IEEE Transactions on Computers*, vol. C-23, no. 1, pp. 90–93, 1974.
- [7] C. Tsutake, K. Takahashi, and T. Fujii, “An efficient compression method for sign information of DCT coefficients via sign retrieval,” *IEEE International Conference on Image Processing*, 2021.
- [8] K. Suzuki, C. Tsutake, K. Takahashi, and T. Fujii, “Compressing sign information in DCT-based image coding via deep sign retrieval,” *ITE Transactions on Media Technology and Applications*, vol. 12, no. 1, pp. 110–122, 2024.
- [9] D. A. Huffman, “A method for the construction of minimum-redundancy codes,” *Resonance*, vol. 11, pp. 91–99, 1952.
- [10] R. Rice and J. Plaunt, “Adaptive variable-length coding for efficient compression of spacecraft television data,” *IEEE Trans. Communication Technology*, vol. 19, no. 6, pp. 889–897, 1971.
- [11] G. N. N. Martin, “Range encoding: an algorithm for removing redundancy from a digitized message,” *Video & Data Recording Conference*, 1979.
- [12] F. Golchin and K. Paliwal, “A context-based adaptive predictor for use in lossless image coding,” *IEEE Region 10 International Conference*, 1997.
- [13] R. Lin, S. Liu, J. Jiang, S. Li, C. Li, and C.-C. J. Kuo, “Recovering sign bits of DCT coefficients in digital images as an optimization problem,” *Journal of Visual Communication and Image Representation*, vol. 98, no. 103992, 2024.
- [14] N. D. Sidiropoulos, P. A. Karakasis, and A. Konar, “Minimizing low-rank models of high-order tensors: hardness, span, tight relaxation, and applications,” *IEEE Transactions on Signal Processing*, vol. 72, pp. 129–142, 2023.

- [15] G. K. Wallace, “The JPEG still picture compression standard,” *Communications of the ACM*, vol. 34, no. 4, pp. 30–44, 1991.
- [16] G. J. Sullivan, J.-R. Ohm, W.-J. Han, and T. Wiegand, “Overview of the high efficiency video coding (HEVC) standard,” *IEEE Transactions on Circuits and Systems for Video Technology*, vol. 22, no. 12, pp. 1649–1668, 2012.
- [17] B. Bross, Y.-K. Wang, Y. Ye, S. Liu, J. Chen, G. J. Sullivan, and J.-R. Ohm, “Overview of the versatile video coding (VVC) standard and its applications,” *IEEE Transactions on Circuits and Systems for Video Technology*, vol. 31, no. 10, pp. 3736–3764, 2021.
- [18] S. Bahmani and J. Romberg, “A flexible convex relaxation for phase retrieval,” *Electronic Journal of Statistics*, vol. 11, no. 2, pp. 5254–5281, 2017.
- [19] T. Goldstein and C. Studer, “PhaseMax: convex phase retrieval via basis pursuit,” *IEEE Transactions on Information Theory*, vol. 64, no. 4, pp. 2675–2689, 2018.
- [20] R. W. Gerchberg and W. O. Saxton, “A practical algorithm for the determination of phase from image and diffraction plane pictures,” *Optik*, vol. 35, pp. 237–246, 1972.
- [21] J. R. Fienup, “Phase retrieval algorithms: a comparison,” *Applied Optics*, vol. 21, no. 15, pp. 2758–2769, 1982.
- [22] M. Frank and P. Wolfe, “An algorithm for quadratic programming,” *Naval Research Logistics Quarterly*, vol. 3, no. 1–2, pp. 95–110, 1956.
- [23] F. Henry and G. Clare, “Residual coefficient sign prediction,” *JVET-D0031*, 2016.
- [24] A. Nakagawa, J. Koyama, K. Kazui, and J. Katto, “Sign information predictive coding of transform coefficients in video compression,” *IEICE Transactions on Information and Systems*, vol. J100-D, no. 9, pp. 819–830, 2017.
- [25] A. Filippov, V. Ruffitskiy, A. Karabutov, and J. Chen, “Residual sign prediction in transform domain for next-generation video coding,” *APSIPA Transactions on Signal and Information Processing*, vol. 8, 2019.
- [26] G. Clare, F. Henry, and J. Jung, “Sign data hiding,” *JCTVC-G271*, 2011.
- [27] G. Bjontegaard, “Calculation of average PSNR differences between RD curves,” *VCEG-M33*, 2001.
- [28] J. Wang, X. Yu, D. He, F. Henry, and G. Clare, “Multiple sign bits hiding for high efficiency video coding,” *IEEE International Conference on Visual Communications and Image Processing*, 2012.
- [29] X. Zhang, O. C. Au, C. Pang, W. Dai, and Y. Guo, “Additional sign bit hiding of transform coefficients in HEVC,” *IEEE International Conference on Multimedia and Expo Workshops*, 2013.
- [30] R. Song, Y. Yuan, Y. Li, and Y. Wang, “Extra sign bit hiding algorithm based on recovery of transform coefficients,” *Circuits, Systems, and Signal Processing*, vol. 37, no. 9, pp. 4128–4135, 2018.

- [31] J. M. Shapiro, “Embedded image coding using zerotrees of wavelet coefficients,” *IEEE Transactions on Signal Processing*, vol. 41, no. 12, pp. 3445–3462, 1993.
- [32] A. Said and W. A. Pearlman, “A new, fast, and efficient image codec based on set partitioning in hierarchical trees,” *IEEE Transactions on Circuits and Systems for Video Technology*, vol. 6, no. 3, pp. 243–250, 1996.
- [33] Challenge on Learned Image Compression, <https://compression.cc>.
- [34] M. Koo, M. Salehifar, J. Lim, and S.-H. Kim, “Low frequency non-separable transform (LFNST),” *Picture Coding Symposium*, 2019.